Switchable Materials

DOI: 10.1002/anie.201208023

Co–NC–W and Fe–NC–W Electron-Transfer Channels for Thermal Bistability in Trimetallic $\{Fe_6Co_3[W(CN)_8]_6\}$ Cyanido-Bridged Cluster**

Robert Podgajny, Szymon Chorazy, Wojciech Nitek, Michał Rams, Anna M. Majcher, Bartosz Marszałek, Jan Żukrowski, Czesław Kapusta, and Barbara Sieklucka**

The design and construction of switchable materials attracts tremendous interest owing to the potential in information storing and processing or molecular sensing.[1–4] The archetypal examples involve a diversity of Fe^{II}-,[5,6] Fe^{III}-[7] or Co^{II}-based[8–10] spin-crossover (SCO) compounds, $Co^{III/II}$-catecholate/semiquinone systems,[1,11] as well as d-d bimetallic and s-d-d trimetallic cyanide-bridged systems revealing charge-transfer-induced spin transitions (CTIST).[12–18] Some of these compounds, for example Prussian blue analogues, are particularly promising from the point of view of photoswitching between nonmagnetic and magnetized (that is, T_B, T_C) states, owing to magnetic coupling through molecular bridges in discrete species[14,15] and extended networks.[17,18] Such bistability also emerged in the magnetochemistry of octacyanidometalates, exploiting metal-to-metal electron transfer in $^{HS}Co^{II}L[W^{V}(CN)_8]^{3-}$ (L = pyrimidine, 4-methylpyridine)[19,20] or canonical SCO in $Fe^{II}L[Nb^{IV}(CN)_8]^{4-}$ extended networks[21] (L = 4-pyridinealdoxime). A magnetic hysteresis loop with a coercivity of 1–3 T were observed in an optically excited low-temperature metastable phase.

As a continuing effort to obtain innovative bistable systems, we explored the simultaneous embedding of Co^{II} and Fe^{II} cations into one octacyanido-bridged coordination skeleton. We have engineered and isolated the novel trimetallic $\{Co^{II}_3Fe^{II}_6[W^{V}(CN)_8]_6(MeOH)_{24}\}\cdot x\,MeOH$ (**1**) material built of nanosized (ca. 20 Å) pentadecanuclear six-capped body-centered cubic $Co_3Fe_6W_6$ clusters with MeOH molecules of crystallization (see the Supporting Information). The $\{M^{II}_9M'^{V}_6(CN)_{48}(L)_{24}\}\cdot n\,solv$ compound family (M = Mn, Co, Ni; M′ = Mo, W; L = blocking ligands; Figure 1) reveal high-

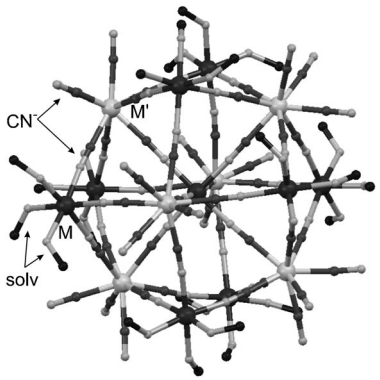

Figure 1. The molecular structure of the $M^{II}_9M'^{V}_6$ clusters. Large dark gray spheres: 3d M′ ions; large pale gray: 4d or 5d M″ ions; small dark gray: C; small pale gray: N; small black: O.

spin ground states[22–26] and SMM (M′ = Ni; L = tmphen, 3,4,7,8-tetramethyl-1,10-phenanthroline)[24] or SMM-like (M = Co, L = MeOH, **2**)[25,26] behavior. Herein, we present for the first time a coexistence and cooperativity between two different active electron-transfer channels in one coordination skeleton, owing to the specific distribution of Co^{II} and Fe^{II} centers at M sites of $\{Co^{II}_3Fe^{II}_6[W^{V}(CN)_8]_6(MeOH)_{24}$ cluster.

The crystals of **1** preserve their morphology, structure, and properties only while stored in mother liquor or in apiezon oil, and thus they were characterized as **1**@MeOH or/and **1**@ap. Compound **1** undergoes a reversible single-crystal-to-single-crystal (SCSC) structural and spin-phase transition with thermal bistability and a hysteresis loop at temperature range 190–210 K. The equilibrium between the high-temperature and low-temperature phases, hereafter denoted as $\mathbf{1}^{HT}$ and $\mathbf{1}^{IT}$, respectively, was characterized by monocrystalline X-ray diffraction,[36] magnetic measurements, IR spectroscopy,

[*] Dr. R. Podgajny, S. Chorazy, Dr. W. Nitek, B. Marszałek, Prof. Dr. B. Sieklucka
Faculty of Chemistry Jagiellonian University
Ingardena 3, 30-060 Kraków (Poland)
E-mail: podgajny@chemia.uj.edu.pl
barbara.sieklucka@uj.edu.pl
Homepage: http://www.chemia.uj.edu.pl/znmm/
Dr. M. Rams, A. M. Majcher
M. Smoluchowski Institute of Physics, Jagiellonian University
Reymonta 4, 30-059 Kraków (Poland)
Dr. J. Żukrowski, Prof. Dr. C. Kapusta
AGH University of Science and Technology, Faculty of Physics and Applied Computer Science
Mickiewicza 30, 30-059 Kraków (Poland)

[**] We thank the Polish National Science Centre (B.S. UMO-2011/01/B/ST5/00716), the International PhD-studies Programme at the Faculty of Chemistry, Jagiellonian University, within the Foundation for Polish Science MPD Programme co-financed by the EU European Regional Development Fund (S.C.). The research was partially carried out with the equipment purchased thanks to the financial support of the European Regional Development Fund in the framework of the Polish Innovation Economy Operational Program (contract no.POIG.02.01.00-12-023/08). We are grateful to Magdalena Wis for the experimental assistance.

Supporting information for this article (complete description of experimental details and characterization, crystallographic and physical characterization of **1**) is available on the WWW under http://dx.doi.org/10.1002/anie.201208023.

^{57}Fe Mössbauer spectroscopy, and differential scanning calorimetry (DSC).

The structural data measured for **1**@ap (250 K, $\mathbf{1}^{HT}$, and 130 K, $\mathbf{1}^{IT}$) and for **1**@MeOH (293 K) indicate that our clusters are topologically identical with those found previously (Figure 1; Supporting Information, Figure S2, Tables S1–S3). In $\mathbf{1}^{HT}$, the M–N distances for the central site are 2.065(7), 2.078(7), and 2.081(7) Å, while for the external sites the mean M–N distances range from 2.119 to 2.137 Å. The mean M–O distances range from 2.109 to 2.125 Å. The M–N distances for the central site are different from those for external sites, falling within the range observed in cyanide-bridged $\{^{HS}Co^{II}[M(CN)_8]^{n-}\}$ assemblies.[25–30] In $\{^{HS}Fe^{II}[M(CN)_8]^{n-}\}$ networks, the Fe–N distances are slightly longer then the Co–N distances.[31] Our data suggest that the central site are occupied by $^{HS}Co^{II}$ cations, while at the external sites two $^{HS}Co^{II}$ cations and six $^{HS}Fe^{II}$ cations are present. The central Co–N distances in **1** are practically identical with the relevant Co–N distances in **2** (2.08 Å), while the M–N distances in **1** are slightly longer the external Co–N distances in **2** (2.09 Å).[25] In $\mathbf{1}^{IT}$, the M–N distances for the central site are significantly decreased to 1.913(7), 1.919(6), and 1.924(7) Å (by ca. 0.16 Å, 7.4 %) compared to $\mathbf{1}^{HT}$. These data indicate strongly that the central M site is occupied by Co^{3+} (Co1; Figure 2 a).[4,12–16] For the external sites, a shortening of the mean M–N distances (to 2.048, 2.069, 2.051, and 2.066 Å) and of the mean M–O distances (to 2.052, 2.075, 2.059, and 2.074 Å) is observed (ca. 0.07 Å, 3.5 %). This effect is less pronounced than for the central Co atom (Figure 2 b) and suggests the presence of statistical mixture of $^{HS}Co^{2+}$ (Co2), $^{HS}Fe^{3+}$, and $^{HS}Fe^{2+}$ spin states in $\mathbf{1}^{IT}$. The presence of $^{LS}Co^{2+}$ is excluded as we do not observe the axial elongation characteristic for this type of six-coordinate moieties.[8–10]

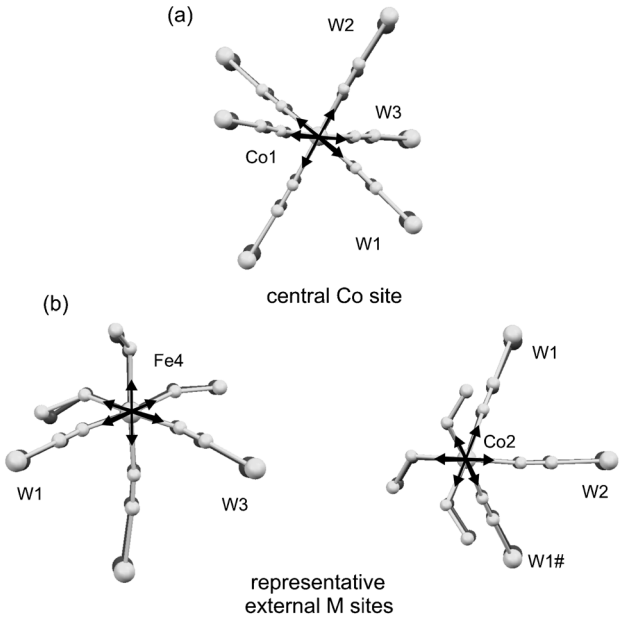

Figure 2. Illustration of local structural alterations between $\mathbf{1}^{HT}$ (pale gray, front layer) and $\mathbf{1}^{IT}$ (dark gray, back layer). Black arrows indicate only the directions of observed change of bond lengths with temperature.

Similarly, the presence of $^{LS}Fe^{II}$ centers can be excluded as M–N distances very weakly match those observed previously in low-spin Fe^{II} complexes[5,6,32] (see also Mössbauer spectra in Figure 4). The relevant M-N-C angles do not change significantly, falling in range 170–177° for $\mathbf{1}^{HT}$ and 167–178° for $\mathbf{1}^{IT}$. The $[W(CN)_8]^{n-}$ units retain their BTP-8 or DD-8 geometry during the thermal transition; no significant modifications in their metric parameters were observed. The Co1–W distances decrease of about 0.13 Å, while in the external part the M′–W distances shorten of ca. 0.07 Å. The transition is accompanied by hydrogen bonds distance reduction by 1.8–4.1 % (Supporting Information, Figure S3) without topological change of clusters arrangement in 3D architecture. Figure 3 presents the quick-scan thermal change of the

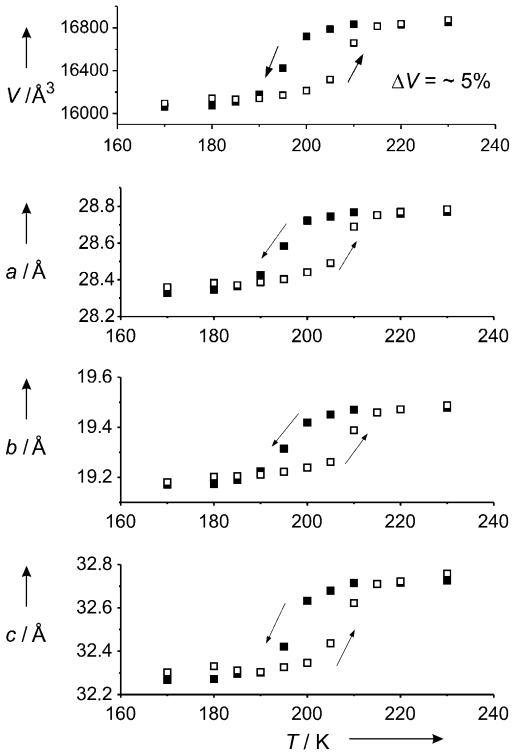

Figure 3. The change of the crystallographic cell parameters for a phase transitions $\mathbf{1}^{HT}\rightarrow\mathbf{1}^{IT}$ (■) and $\mathbf{1}^{IT}\rightarrow\mathbf{1}^{HT}$ (□).

crystallographic cell parameters measured in decreasing and in increasing temperature mode. All periods shorten significantly during the transition from $\mathbf{1}^{HT}$ to $\mathbf{1}^{IT}$, while the space group *C*2/*c* and the angle β are retained. This results in cell volume compression from about 16900 Å^3 to about 16100 Å^3, or 5 %. Upon heating, the hysteresis closes with the critical temperatures $T_{c\downarrow} = 194$ K and $T_{c\uparrow} = 207$ K. Summarizing the presented structural features, we conclude that within the dynamic 3D supramolecular architecture of **1** the $Co_3Fe_6W_6$ clusters serve as individual nanosized dynamic nodes composed of bond-flexible $[M(\mu\text{-}NC)_6]$ and $[M(\mu\text{-}NC)_3(MeOH)_3]$ units as well as of definitely rigid $[W(CN)_8]^{n-}$ moieties.

^{57}Fe Mössbauer spectrum measured for **1**@ap at 298 K was deconvoluted into three doublets indisputably assignable to $^{HS}Fe^{II}$ centers, while at 80 K a strong doublet assignable to

$^{HS}Fe^{III}$ and a weak doublet characteristic for $^{HS}Fe^{II}$ were found, with the relative intensity of $^{HS}Fe^{III}$ and $^{HS}Fe^{II}$ signals close to 5:1 (Figure 4; Supporting Information, Table S4). The Mössbauer spectra points to the composition $(^{HS}Co^{II})_3(^{HS}Fe^{II})_6(W^V)_6$ of $\mathbf{1^{HT}}$ and $(^{LS}Co^{III})(^{HS}Co^{II})_2(^{HS}Fe^{III})_4(^{HS}Fe^{II})_2(W^V)(W^{IV})_5$ of $\mathbf{1^{IT}}$.

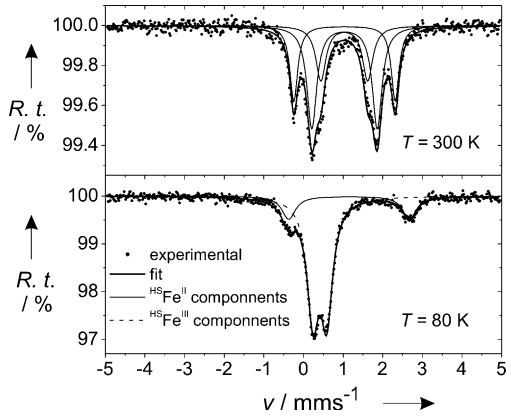

Figure 4. The Mössbauer spectra of $\mathbf{1^{HT}}$ (top) and $\mathbf{1^{IT}}$ (bottom).

The ν(CN) IR pattern for **1**@ap at 298 K reveals the 2216, 2188, 2165, 2152, 2115 cm^{-1} peak set, while at 150 K the 2210, 2193, 2154, 2118, 2075 cm^{-1} peak set was detected (Figure 5).

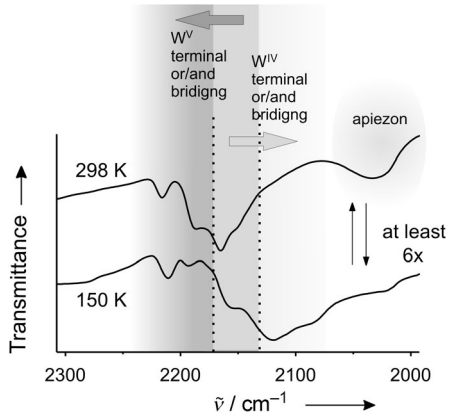

Figure 5. A multiple reversibility of IR spectra for $\mathbf{1^{HT}}$ and $\mathbf{1^{IT}}$.

The detailed evolution of ν(CN) IR spectra with decreasing and increasing temperature is presented in the Supporting Information, Figure S4. Our data indicate the presence of W^V centers in $\mathbf{1^{HT}}$ and the mixture of W^V and W^{IV} centers in $\mathbf{1^{IT}}$.[19,20,33] This conforms to the presence of Co^{II} and Fe^{II} ions in $\mathbf{1^{HT}}$ and Co^{III}, Co^{II}, Fe^{II}, and Fe^{III} ions suggested for $\mathbf{1^{IT}}$, respectively. Both techniques reveals perfect reversibility of the signal after subsequent heating to 298 K.

Magnetic $\chi_M T(T)$ and $M(H)$ curves were measured for **1**@MeOH (Figure 6; Supporting Information, Figure S5). The carefully corrected $\chi_M T(T)$ signal has the value of 34.5 $cm^3 K mol^{-1}$ at 298 K, which is in a good agreement with 34.2 $cm^3 K mol^{-1}$ expected for a $(^{HS}Co^{II})_3(^{HS}Fe^{II})_6(W^V)_6$

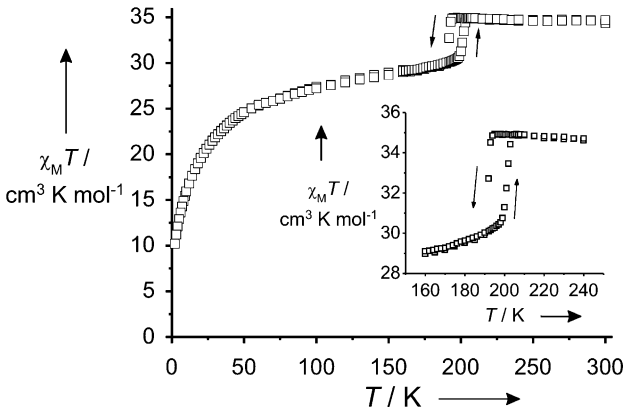

Figure 6. Magnetic characteristics for **1**: the $\chi_M T(T)$ curve for **1** (H_{dc} = 1 kOe). Inset: a thermal hysteresis loop.

composition in $\mathbf{1^{HT}}$.[27,29,31,34,35] The cooling–heating-mode measurement reveals the presence of reversible signal with thermal hysteresis described by the critical temperatures $T_{c\downarrow} = 192$ K and $T_{c\uparrow} = 202$ K. The change of $\chi_M T$ of about 5.0 $cm^3 K mol^{-1}$ in this region is in good agreement with the sum of one contribution from the $^{HS}Co^{II}$–NC–$W^V \rightleftarrows {}^{LS}Co^{III}$–NC–$W^{IV}$ equilibrium (ca. 3.8 $cm^3 K mol^{-1}$) and four contributions from the $^{HS}Fe^{II}$–NC–$W^V \rightleftarrows {}^{HS}Fe^{III}$–NC–$W^{IV}$ equilibrium (ca. 1.0 $cm^3 K mol^{-1}$) per one $Co_3Fe_6W_6$ cluster. In the $\mathbf{1^{IT}}$ phase, the magnetic exchange is almost cancelled (contrary to that observed for the reference compound **2**) owing to the appearance of diamagnetic centers, and a signal should be interpreted in terms of single-ion properties and weak intermolecular interactions. A more detailed description and evaluation of magnetic curves is included in the Supporting Information, Figure S5. The differential scanning calorimetry (DSC) signals measured for **1**@ap reveal a positive peak at 194 K in the cooling mode and a negative peak at 204 K in the heating mode confirming the first-order hysteretic transition. (Supporting Information, Figure S6).

We have shown that reversible hysteretic SCSC transition between $\mathbf{1^{HT}}$ and $\mathbf{1^{IT}}$ occurs for trimetallic $Co^{II}{}_3Fe^{II}{}_6[W^V(CN)_8]_6$ clusters of **1** with $T_{c\downarrow} \approx 193$ K and $T_{c\uparrow} \approx 207$ K, both for **1**@ap and **1**@MeOH samples. All types of d centers are simultaneously involved in structural and spin-state $\mathbf{1^{HT}} \rightleftarrows \mathbf{1^{IT}}$ equilibria: the $W^V \rightleftarrows W^{IV}$ equilibrium is undoubtedly accompanied by $^{HS}Co^{II} \rightleftarrows {}^{LS}Co^{III}$ and $^{HS}Fe^{II} \rightleftarrows {}^{HS}Fe^{III}$ equilibria. This indicates that in **1**, a unique thermal CTIST is involved that *simultaneously* employs two different electron transfer channels, $^{HS}Co^{II}$–NC–$W^V \rightleftarrows {}^{LS}Co^{III}$–NC–$W^{IV}$ and $^{HS}Fe^{II}$–NC–$W^V \rightleftarrows {}^{HS}Fe^{III}$–NC–$W^{IV}$ (Figure 7). The former was observed before in 3D {Co-L-$[W(CN)_8]^{n-}$} coordination networks,[19,20] while the W^V;$^{HS}Fe^{II} \rightleftarrows W^{IV}$;$^{HS}Fe^{III}$ electron transfer is reported for the first time. No phase transition was found for the compound **2** composed of Co_9W_6 clusters,[25,26] and therefore we correlate the phenomenon of CTIST in **1** with replacement of six $^{HS}Co^{II}$ in Co_9W_6 clusters by six $^{HS}Fe^{II}$ centers. This resulted in a slight increase of average external M–N bond lengths from 2.09 Å in **2** to 2.12–2.14 Å in **1**.[25] It is plausible that the elongation of M–N bonds produces a structural tension to the cluster skeleton, which could act as a driving force for structural thermal transformation. The subsequent

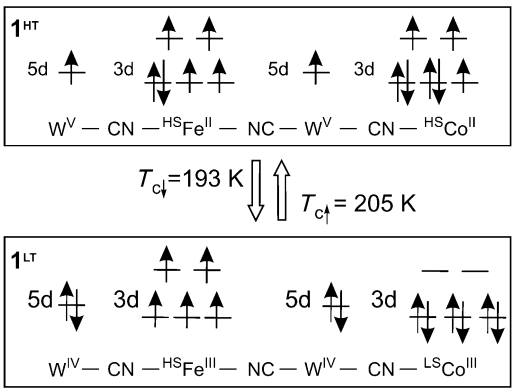

Figure 7. The modification of valence electronic structure for a phase transitions $\mathbf{1}^{HT} \rightarrow \mathbf{1}^{IT}$.

$^{HS}Co^{II} \rightarrow {}^{LS}Co^{III}$ and $^{HS}Fe^{II} \rightarrow {}^{HS}Fe^{III}$ spin transitions result in a decrease in the Co–N bond lengths of about 0.16 Å in the central Co moiety, and in M–N and M–O bond-length shortening of about 0.07 Å in the external 3d ion moieties. The $[M(CN)_8]^{n-}$ moieties remain unchanged during the phase transition and serve only as a rigid linkers for cluster expansion/compression. The intercluster contacts are controlled by hydrogen bonds, which contribute by easily shortening and elongating without topological changes to the dynamic character of **1** (Supporting Information, Figure S3).

In summary, we have shown that the nanosized $\{M^{II}_9M'^{V}_6(CN)_{48}(L)_{24}\}$ cluster may serve as an individual molecular platform for observation of thermal bistability owing to strong internal cooperative effects. To the best of our knowledge, we present for the first time a coexistence of two active electron-transfer channels in one trimetallic material. The presence of Co^{II} ions at the central M site and combination of Co^{II} and Fe^{II} centers at the external M sites creates unique conditions for observation of hysteretic CTIST transition. Our studies opens a novel research pathway on a family of $Fe_xCo_{9-x}[W(CN)_8]_6$ ($x = 1$–9) clusters. Several points could be addressed in the future: searching for the boundary where high-spin molecules and thermal bistability systems come together, functionalization and organization of mixed clusters using organic ligands, optical excitation of metastable high-spin states towards novel discrete high spin systems, and also the bistability within a frame of trimetallic $Fe_xCo_y[M(CN)_8]_z$ coordination network.

Received: October 4, 2012
Published online: November 26, 2012

Keywords: charge transfer · cluster compounds · cooperative effects · cyanides · trimetallic complexes

[1] O. Sato, J. Tao, Y.-Z. Zhang, *Angew. Chem.* **2007**, *119*, 2200–2236; *Angew. Chem. Int. Ed.* **2007**, *46*, 2152–2187.
[2] M. A. Halcrow, *Chem. Soc. Rev.* **2011**, *40*, 4119–4142.
[3] J. Tao, R.-J. Wei, R.-B. Huang, L.-S. Zheng, *Chem. Soc. Rev.* **2012**, *41*, 703–737.
[4] A. Bleuzen, V. Marvaud, C. Mathoniere, B. Sieklucka, M. Verdaguer, *Inorg. Chem.* **2009**, *48*, 3453–3466.
[5] P. Chakraborty, R. Bronisz, C. Besnard, L. Guénée, P. Pattison, A. Hauser, *J. Am. Chem. Soc.* **2012**, *134*, 4049–4052.
[6] M. C. Muñoz, J. A. Real, *Coord. Chem. Rev.* **2011**, *255*, 2068–2093.
[7] M. Nihei, T. Shiga, Y. Maeda, H. Oshio, *Coord. Chem. Rev.* **2007**, *251*, 2606–2621.
[8] K. Bhar, S. Khan, J. Sánchez Costa, J. Ribas, O. Roubeau, P. Mitra, B. Kumar Ghosh, *Angew. Chem.* **2012**, *124*, 2184–2187; *Angew. Chem. Int. Ed.* **2012**, *51*, 2142–2145.
[9] M. G. Cowan, J. Olguín, S. Narayanaswamy, J. L. Tallon, S. Brooker, *J. Am. Chem. Soc.* **2012**, *134*, 2892–2894.
[10] S. Hayami, D. Urakami, Y. Kojima, H. Yoshizaki, Y. Yamamoto, K. Kato, A. Fuyuhiro, S. Kawata, K. Inoue, *Inorg. Chem.* **2010**, *49*, 1428–1432.
[11] D. Kiriya, H.-C. Chang, K. Nakamura, D. Tanaka, K. Yoneda, S. Kitagawa, *Chem. Mater.* **2009**, *21*, 1980–1988.
[12] T. Liu, D.-P. Dong, S. Kanegawa, S. Kang, O. Sato, Y. Shiota, K. Yoshizawa, S. Hayami, S. Wu, C. He, C.-Y. Duan, *Angew. Chem.* **2012**, *124*, 4443–4446; *Angew. Chem. Int. Ed.* **2012**, *51*, 4367–4370.
[13] M. Nihei, Y. Sekine, N. Suganami, K. Nakazawa, A. Nakao, H. Nakao, Y. Murakami, H. Oshio, *J. Am. Chem. Soc.* **2011**, *133*, 3592–3600.
[14] M. Nihei, Y. Okamoto, Y. Sekine, N. Hoshino, T. Shiga, I. P.-C. Liu, H. Oshio, *Angew. Chem.* **2012**, *124*, 6467–6470; *Angew. Chem. Int. Ed.* **2012**, *51*, 6361–6364.
[15] D.-P. Dong, T. Liu, S. Kanegawa, S. Kang, O. Sato, C. He, C.-Y. Duan, *Angew. Chem.* **2012**, *124*, 5209–5213; *Angew. Chem. Int. Ed.* **2012**, *51*, 5119–5123.
[16] D. Li, R. Clérac, O. Roubeau, E. Harté, C. Mathonière, R. Le Bris, S. M. Holmes, *J. Am. Chem. Soc.* **2008**, *130*, 252–258.
[17] N. Shimamoto, S. Ohkoshi, O. Sato, K. Hashimoto, *Inorg. Chem.* **2002**, *41*, 678–684.
[18] C. Avendano, M. G. Hilfiger, A. Prosvirin, C. Sanders, D. Stepien, K. R. Dunbar, *J. Am. Chem. Soc.* **2010**, *132*, 13123–13125.
[19] S. Ohkoshi, Y. Hamada, T. Matsuda, Y. Tsunobuchi, H. Tokoro, *Chem. Mater.* **2008**, *20*, 3048–3054.
[20] N. Ozaki, H. Tokoro, Y. Hamada, A. Namai, T. Matsuda, S. Kaneko, S. Ohkoshi, *Adv. Funct. Mater.* **2012**, *22*, 2089–2093.
[21] S. Ohkoshi, K. Imoto, Y. Tsunobuchi, S. Takano, H. Tokoro, *Nat. Chem.* **2011**, *3*, 564–569.
[22] Z. J. Zhong, H. Seino, Y. Mizobe, M. Hidai, A. Fujishima, S. Ohkoshi, K. Hashimoto, *J. Am. Chem. Soc.* **2000**, *122*, 2952–2953.
[23] F. Bonadio, M. Gross, H. Stoeckli-Evans, S. Decurtins, *Inorg. Chem.* **2002**, *41*, 5891–5896.
[24] M. G. Hilfiger, H. Zhao, A. Prosvirin, W. Wernsdorfer, K. R. Dunbar, *Dalton Trans.* **2009**, 5155–5163.
[25] Y. Song, P. Zhang, X.-M. Ren, X.-F. Shen, Y.-Z. Li, X.-Z. You, *J. Am. Chem. Soc.* **2005**, *127*, 3708–3709.
[26] D. E. Freedman, M. V. Bennett, J. R. Long, *Dalton Trans.* **2006**, 2829–2834.
[27] J. M. Herrera, A. Bleuzen, Y. Dromzée, M. Julve, F. Lloret, M. Verdaguer, *Inorg. Chem.* **2003**, *42*, 7052–7059.
[28] D. Li, L. Zheng, Y. Zhang, J. Huang, S. Gao, W. Tang, *Inorg. Chem.* **2003**, *42*, 6123–6129.
[29] D. Pinkowicz, R. Pełka, O. Drath, W. Nitek, M. Bałanda, A. M. Majcher, G. Poneti, B. Sieklucka, *Inorg. Chem.* **2010**, *49*, 7565–7576.
[30] J. Wang, Y.-L. Xu, H.-B. Zhou, H.-S. Wang, X.-J. Song, Y. Song, X.-Z. You, *Dalton Trans.* **2010**, *39*, 3489–3494.
[31] D. Pinkowicz, R. Podgajny, R. Pełka, W. Nitek, M. Bałanda, M. Makarewicz, M. Czapla, J. Żukrowski, C. Kapusta, D. Zając, B. Sieklucka, *Dalton Trans.* **2009**, 7771–7777.
[32] D. W. Blakesley, S. C. Payne, K. S. Hagen, *Inorg. Chem.* **2000**, *39*, 1979–1989.

[33] R. Podgajny, T. Korzeniak, K. Stadnicka, Y. Dromzée, N. W. Alcock, W. Errington, K. Kruczała, M. Bałanda, T. J. Kemp, M. Verdaguer, B. Sieklucka, *Dalton Trans.* **2003**, 3458 – 3468.
[34] F. Lloret, M. Julve, J. Cano, R. Ruiz-García, E. Pardo, *Inorg. Chim. Acta* **2008**, *361*, 3432 – 3445.
[35] M. S. Shongwe, B. A. Al-Rashdi, H. Adams, M. J. Morris, M. Mikuriya, G. R. Hearne, *Inorg. Chem.* **2007**, *46*, 9558 – 9568.
[36] CCDC 904167, 904168, and 904169 contains the supplementary crystallographic data for this paper. These data can be obtained free of charge from The Cambridge Crystallographic Data Centre via www.ccdc.cam.ac.uk/data_request/cif.

